# Rock cliffs hazard analysis based on remote geostructural surveys: The Campione del Garda case study (Lake Garda, Northern Italy)



*Published version:*

DOI:10.1016/j.geomorph.2010.10.009



(Article begins on next page)

A.M. Ferrero, M. Migliazza, R. Roncella, A. Segalini, (2011) Rock cliffs hazard analysis based on remote geostructural surveys: The Campione del Garda case study (Lake Garda, Northern Italy), Geomorphology, Volume 125, Issue 4, 15 February 2011, Pages 457-471, ISSN 0169-555X,

DOI: 10.1016/j.geomorph.2010.10.009.

Title

# Rock cliffs hazard analysis based on remote geostructural surveys: the Campione del Garda case study (Lake Garda, Northern Italy)

Authors:

**Ferrero, A.M., Migliazza, M., Roncella, R., Segalini, A.**

Affiliation:

Department of Civil, Environmental and Territory Engineer and Architecture (DICATeA) – University of Parma - V.le Usberti 181/a - 43124 Parma - Italy

Correspondance to:

Prof. Andrea Segalini
c/o Dept. Of Civil, Environmental and Territory Engineering and Architecture (DICATeA)
University of Parma
V.le Usberti 181/a
43124 Parma
Italy

Tel. +39.0521.905952
Fax +39.0521.905924
Email: andrea.segalini@unipr.it

## Abstract

The town of Campione del Garda (located on the west coast of Lake Garda) and its access road have been historically subject to rockfall phenomena with risk for public security in several areas of the coast.. This paper presents a study devoted to the determination of risk for coastal cliffs and the design of mitigation measures. Our study was based on statistical rockfall analysis performed with a commercial code and on stability analysis of rock slopes based on the key block method. Hazard from block kinematics and rock-slope failure are coupled by applying the Rockfall Hazard Assessment Procedure (RHAP). Because of the huge dimensions of the slope, its morphology and the geostructural survey were particularly complicated and demanding. For these reasons, noncontact measurement methods, based on aerial photogrammetry by helicopter, were adopted. A special software program, developed by the authors, was applied for discontinuity identification and for their orientation measurements. The potentially of aerial photogrammetic survey in rock mechanic application and its improvement in the rock mass knowledge is analysed in the article.

*Keywords*: rockfall hazard; remote geostructural survey; risk analysis; Campione del Garda; Northern Italy.

## 1 Introduction

The rock fall phenomenon usually involves limited volumes of rock but it represents an element of relevant hazard since it is a fast, sudden and, within the Italian territory is also a widespread phenomenon. This problem assumes higher significance in the areas where urban settlements and infrastructures have been developed in close proximity of rock cliffs.

Typical is the Lake Garda case, the widest Italian fresh water basin, located at the Alpine Arch base, among the provinces of Brescia, Verona, Mantova and Trento.

The lake north-western shore is characterized by high and wide sub-vertical rock cliffs where an important tourism activity is located giving to the lake shore an interesting economical importance.

The study regards the rock slope that overlooks the Campione del Garda inhabited shore, on the west bank of the lake, frequently subjected to rock fall phenomena (Fig. 1).

The occurrence of several rock fall events drove the public administration to take steps in order to improve the safety of this area characterized by an high risk increased by the presence of a well developed tourist activity. Due to the morphological settings of the rock walls, the use of defence systems to prevent block detachment, appeared not achievable so in order to choose and define the most appropriate defence system an hazard assessment procedure was needed.

## 2 Geological setting

The surveyed area is, from the geological point of view, part of the Subalpine structural domain, located in the central sector of the Southern Alps and constituted by folds and thrusts having a primary direction E-W.

The main geological unit surfacing in the studied area is the Main dolomite constituted by a succession of stratified dolomite limestones sometime marly limestone and thin marl and bituminous layers followed by the proper dolomite unit in its grey, white and pink facies.

This Subalpine structural sector is formed by a single and relict palaeographic element: the Lumbard Mesozoic basin which is characterized by homogeneous style of deformation, outcrop shortening and wrinkling age. The studied area involves the eastern portion of such domain, where the stratigraphic series are considerably thinner than those usually encountered in the domain.

Along the Eastern shore of the Garda lake, stratigraphic sequences pertaining to the Veneta Platform Domain are outcropping (mainly constituted by limestones of shallow or extremely shallow sea formation); this Platform is divided from the Lumbard Basin (mainly constituted by limestone and silica deposits of open and deep sea formation) by the Ballino-Garda line: this line represents the tectonic Mesozoic scarp, formed by normal or vertical faults of Jurassic-Cretaceous age that significantly lowered the western sector in respect of the eastern.

Such tectonic line is part of a general process of relaxation that involved the whole domain starting from the Late Triassic/Lower Jurassic up to the Lower Cretaceous and determined a structural fragmentation of the domain in a series of structural ups and dows (block faulting, Cassinis e Vercesi, 1982); this events where combined with an irregular subsidence, which controlled the sedimentation characteristics. The Alpine orogeny started from the Central/Upper Cretaceous with compressive tectonic which carried on in three distinct phases, interspaced by periods of tectonic stasis.

The study area is constituted by structural elements that formed or reactivate during the last phase of the Alpine orogeny, which took place from 29-25 Ma and 10-7 Ma.

In this zone a continuous stratigraphic sequence of sedimentary limestone units of ages between the Upper Trias (Norico) and the Eocene can be recognized; frequently, however, this sequence is not regular. The various Units outcropping in the study area, from the oldest to the youngest, are constituted by an alternation of dolomia limestone and compact and crystalline limestones of greyish-white colour (Castellarin, 1982).

## 3 Method of study

Rockfall phenomena are frequently recorded in coastal areas where high cliffs are present. Where coastal areas are densely inhabited, an intrinsic hazard condition can become a high risk condition

(Fig. 1). Risk assessment is an important tool for designing mitigation measures and for planning rational land use in these areas. The absolute risk assessment, however, requires analysis in terms of probability of occurrence based on systematic recording of instability phenomena that are seldom available. For zonation purposes, however, expressing hazard, and thus risk, in relative terms (Canuti et al., 1998) is possible.

Many researchers have been dedicated to improve rockfall susceptibility at local and larger scale (Agliardi and Crosta, 2002; Crosta and Agliardi, 2003; Jubyedoff et al., 2005; Copons and Vilaplana, 2008; Frattini et al. 2008) with different aims and field of applicability: in environmental mining to reduce accidents in quarries (Alejano et al., 2008), to solve rockfall problems along public roads (Schweigt et al., 2003; Guzzetti et al., 2004), or to generally improve land use planning (Abellán et al., 2006).

Many of these works outline the importance of improving forecast reliability by developing more powerful modelling tools (Agliadi and Crosta, 2003; Dorren, 2003) and by a more accurate geotechnical and geomechanical characterization of the slopes (Schwegh et al., 2003). The rock mass structure evaluation is important for determining the detachment zones and kinds but also the rock block volume and shape. The importance of a better estimation of the block features is also needed to forecast the block runoff and its velocity, energy, etc. (Okura et al., 2000; Dussage et al., 2002) . These results also have been validated by applying numerical and physical models based on a series of probabilistic analysis to take rock mass variability into account and on in situ tests (Giani et al., 2004).

This paper presents the application of an hazard and risk zonation methodology called Rockfall Hazard Assessment Procedure (RHAP) (Mazzoccola and Sciesa, 2001) based on an aerial photogrammetrical survey done by helicopter and elaborated to obtain both slope geometry and geomechanical information. Due to the extremely large slope dimensions (1500 m wide and 500 m tall), a special noncontact procedure based on aerial photogrammetry was needed for a more detailed and precise rock mass characterization.

A geostructural survey devoted to a systematic and quantitative description of rock discontinuities is a fundamental part of the study of the stability conditions of a rock mass. Traditionally, surveys were performed with a geological compass, measuring dip and dip direction directly on the discontinuity. This method was difficult because discontinuities or even rock faces themselves cannot be easily accessed, and the dimension is so large that data acquisition on site would have been long and expensive.

An alternative to traditional surveys, in many cases capable of overcoming these problems, is to derive dip and dip direction, as well as the location of the discontinuities, from a highly detailed topographic survey—i.e., by measuring a dense "point cloud" on the rock surface. If a set of points surveyed on a particular discontinuity is selected, dip and dip direction can be computed directly from the equation of the best fitting plane. Therefore, the survey will provide not only the slope topography but also the identification of the discontinuities in terms of position on the slope and orientation, spacing, persistence, and joint hierarchy.

To obtain the required results, interactive or automated software tools are necessary to allow the efficient selection from the point clouds of the discontinuities. The software utilized in this work is based on the RANSAC algorithm (Fisher and Bolles, 1981) that allows the semiautomatic segmentation of a point cloud to extract the discontinuities of a rock slope; the algorithm is implemented in an interactive software program that takes a point cloud input as well as oriented images. By contouring on the image, an area with one or several discontinuities, their position, dip, dip direction are automatically computed (Ferrero et al., 2009).

Once the topography of the slope and the geostructure are known, a kinematic analysis can be obtained. Among other factors, the blocky nature of the rock mass strongly influences the stability conditions of the slope; consequently, a method such as the key block method, which takes the discontinuities into account, is applied. The block paths are then computed by applying the Colorado Rockfall Simulation Program (CRSP) code (Pfeiffer and Bowen, 1989), which determines the rock block path on the basis of the lumped mass assumption (the block is considered as a mass point) in a statistical manner by simulating several different scenarios for each section.

## 4 Hazard and risk assessment

The RHAP expeditious method of hazard evaluation allows for the zonation of the territory on a detailed scale, referring to restricted and clearly defined classification of hazard and relative risk. The extrapolation from hazard to risk has been presented in a simplified manner, as the priority of the study has concentrated on hazard definition because of its complexity. The hazard zonation resulting from the application of such procedures is related strictly to the investigated site and is not comparable with other sites. The reason for this is that each investigated site is divided into areas ranging from low to high hazard levels, independently from the absolute hazard values.

A rigorous hazard evaluation should consider the intensity of the phenomenon, which in turn is related to the volume of the involved blocks, the traveling velocity and the probability that the event should again be evaluated on the basis of a case history of the events in order to define their recurrence. Often this is not practicable in an expeditious methodology, and for this reason only semiquantitative parameters (block volume and shape, travelling velocity) have been chosen for zonation.

## 4.1 Rockfall hazard zonation

The RHAP procedure adopted, has been suggested by the competent local authority (Lombardia region) responsible of the land security and it represents an evolution of the Rockfall hazard Rating System (RHRS) developed by the US Transportation Research Board. Both the method are applicable when the fall involves single block having a maximum volume of 1000 $m^3$ and are composed of several phases. A complete description of the methods is given by Pierson et al (1990) and Mazzocola and Sciesa (2001). In the following, the main features of the RHAP method are reported for an easier understanding of the work.

The first step is dedicated to the identification of rock-slope sectors with potential rockfalls. Following this identification, a delimitation of homogeneous areas (Fig. 2) is carried out on the basis of the geomechanical characteristics of the rock mass, of the slope morphology, and of the presence of defensive systems. These features are then used for the numerical modeling of the phenomenon.

For each homogeneous area so defined, one or more descent trajectories are chosen on the basis of observation of the topographic map for the site (15 sections reported in Fig. 2). Along such trajectories the numerical simulations are performed using stochastic models integrating geomechanical surveys and observation of the debris accumulations at the slope toe.

The rockfall numerical simulation (by means of kinematic and/or dynamic models) should be performed in consideration of the block-detachment zone: the block volume, evaluated using the geomechanical surveys. The block shape and the restitution and roughness coefficients of the slope are also considered: these should be evaluated through a detailed survey of the rockfall trajectories.

As this analysis has an important statistical content, performing several rockfall simulations to decrease the bias is necessary. On the bases of the rockfall numerical analysis results, a preliminary longitudinal zonation of the rockfall trajectories should be done, dividing the entire path into three different zones:

(i) transit and stopping of 70% of the blocks;

(ii) stopping of 95% of the blocks; and

(iii)stopping of 100% of the blocks.

These percentages should be evaluated on the total amount of the simulations that were carried out, along each trajectory, on the modal blocks of every considered shape, considering the most unfavorable longitudinal zonation. The relative hazard classes — (a), (b), (c) — are assigned to these zones which are related to rate 4, 3 and 2, respectively. In addition, in this preliminary zonation, an area limited by the block's maximum traveled distance is also delimited and assigned a low hazard value of 1.

Subsequently, the event probability is evaluated for each of the homogeneous areas by defining the block detachment propension for each sector. For this purpose, the rock front must be subdivided using a square net with dimensions of 20 m (Fig. 3), determined on the base of the geomechanical complexity of the homogeneous area and the rock-front extension.

Subsequently, the number of the following 5 instability elements were observed: fracture apertures, block tilting, fracture intensity areas, surface weathering and water presence;. For each of $N_{tot}$ cells the number of instability elements ($n_i$) were determined. Then the percentage of activity was determined for each homogeneous area as follow:

$$activity\% = \frac{5 * N_{tot}}{\sum_{1}^{N_{tot}} n_i} \cdot 100$$

On the basis of the activity percentage, the homogeneous areas are assigned to three groups of high (>70%), medium(35%÷70%), and low (<35%) relative activity. The homogeneous areas where the blocks are rolling or stopping are often partially or completely overlapping; in such cases the map representation should be made in such a way as to highlight those areas having higher degrees of activity, placed upon others with lower degrees of activity. The final hazard zonation is obtained using the values of relative hazard classes for the block transit and accumulation areas, which will be increased by 1, kept equal, or reduced by 1 depending on the activity degree of the overlooking rock slope. Five hazard classes are therefore defined with values increasing from H1 to H5.

## 4.2 Risk zonation

Once the hazard has been defined, the risk assessment and zonation can be performed.

In order to carry out a rigorous classification of the risk, one should evaluate the vulnerability through a comparison with the intensity of the phenomenon and subsequently combine it with both the hazard and the economic evaluation (which would allow for the assessment of the pending damage). In the particular procedure described in the previous section, the phenomenon intensity has already been taken into account for the evaluation of the hazard; the risk assessment is performed more easily by combining the exposed risk elements with the hazard classes.

## 5 Topographic survey

No contact topographic methods have been recently applied to improve the geostructural survey. A full description of the method is given in Ferrero et al. (2009).

Photogrammetry delivers three-dimensional coordinates of points with predictable accuracy from stereo or multiple images (i.e., from images of the same scene taken from different standpoints). The accuracy of the coordinates depends on a number of factors, which must be accounted for in designing the three stages of any photogrammetric survey: camera calibration, image orientation, and object restitution.

Using feature-based image matching and structure from motion (Roncella et al., 2005; Birch, 2006), tie points can be extracted and matched automatically; therefore, image orientation can be obtained without any manual measurement. Orientation parameters can also be determined directly by fixing a Global Positioning System (GPS) receiver, integrated with an Inertial Measurement Unit (IMU) to the camera (Vallet et al., 2000); in this case, no Ground Control Point (GCP) are necessary.

Object restitution can be executed manually by an operator or automatically. The first option exploits the ability of the operator to select the minimum number of points necessary for reliable identification of a discontinuity plane. The latter option exploits the capabilities of image-matching algorithms, such as least-squares matching (Grun, 1985), to compute several thousand points in seconds. Camera stations and camera focal length must be chosen to ensure appropriate image resolution for the object; depending on site characteristics, terrestrial or aerial photogrammetry can be used relative to the precision needed. In this specific case, helicopter aerial photogrammetry was used.

One point every 10 cm, with a precision of 5 cm, was required for all rock slopes. Six representative areas of 10 m× 10 m were identified as particularly interesting from the geomechanical point of view, and one point every 1–2 cm was measured. A focal length of 18 mm for a DTM (digital terrain model) of 10 cm spacing and a focal length of 50 mm for detailed areas were adopted. The shooting distance was about 100 m with parallel flying strips to obtain 50% of superimposition. Fig. 4 shows the shooting position during the flight.

## 5.1 Interactive extraction of planar surfaces with RockScan

A software package named RockScan has been developed to allow the interactive extraction of planes based on the RANSAC procedure. The user loads an oriented image of the rock slope and the point cloud in the background. Through a graphical user interface, Regions of Interest (ROI) enclosing one or more discontinuities can be selected drawing polylines in the image; the corresponding points are selected in the point cloud and input to the RANSAC. For each ROI, dip and dip direction of all the identified planes are computed.

With respect to processing parameters, with a few trials the user can adapt the acceptance threshold in RANSAC to account for measurement noise, resolution of the point cloud, and roughness of the discontinuity surface; values in the range of 5 to 20 cm were found to be appropriate in the cases given later. The discontinuity parameters are output in an appropriate format for the ensuing geometric modeling of the rock face. Figures 5 and 6 show orthophotos of the south and north cliffs, with the detailed areas shown in Fig. 7.

## 5.2 Geostructural survey

A geostructural survey was performed in detailed areas indicated in figures 5 and 6 by analyzing 1445 planes distributed in the six areas (Fig. 7).

Statistical evaluation of the rock-mass structure was then performed by use of the commercial code DIPS (Rockscience) to determine the joint sets in each area. Fig. 8 shows the stereogram reproduction of the isocurves of measured poles and joint sets identified in each zone.

For each detailed zone, virtual scanlines were constructed in order to measure the discontinuity spacing and relative frequency distribution, as shown in Fig. 9, that also shows exponential interpolation curves, as evidenced in the literature (Priest and Hudson, 1981). The homogeneity of two observed zones is noteworthy for joining together data belonging to the south and north slopes.

On the south slope, four detailed areas were identified: zones 1, 2, 3, and 4 in figures 5 and 7. Also, 923 planes were measured in terms of orientation and spacing. Four joint sets (K1, K2, K3, and K4) were identified, as reported in Fig.8.

On the North slope, 218 poles were measured in two detailed zones (zones 5, 6 in Figure 6 and 7) where, again, four joint sets were identified (K1, K2, K3, K4). Orientation data are reported in Tab. 1, considering that average spacing was estimated to be equal to 0.20 m, varying between 0.05 and 0.59 m. As shown in Table 1, the slopes exhibit a similar structure characterized by bedding plane (K1) and three subvertical joint sets.

# 6 Analysis of potential instability phenomena

The stability of the rock slopes is due mainly to the rock-mass structure. The orientation of the discontinuities in relation to that of the slope determines the kinetic potential of the rock blocks to move along the discontinuity planes or their intersections. Limit equilibrium methods (LEM) therefore can be applied to verify the stability condition of possibly unstable blocks. Among others, the key block theory can be applied to identify critical blocks as a result of discontinuity intersections in a rock mass free along defined surfaces. The critical blocks can liberate other blocks that were previously restrained, once they move or detach from the rock mass.

## 6.1 Key block theory

The essential part of the key block theory is the analysis of the discontinuity system in conjunction with the free surfaces. Intersecting discontinuities, these surfaces originate solids of variable shape that, in connection with either externally applied forces or mobilizable strengths, can leave free surfaces and be in critical stability conditions. The theory aims to identify the critical blocks that, in the absence of appropriate contrast, release other blocks near the digging and trigger the collapse of the rock structure. The block in the most dangerous position, the first to be released, is defined as the key block. If the potentially dangerous block (key block) is identified before movement begins, and if its stability is assured, then the other blocks will not move. The method can be implemented either with a vector calculus or a graphic process. The graphic process uses equiangular stereographic projection. This kind of projection represents a particular perspective form in which a single projection point exists, which coincides with one of the two projection sphere poles, in this case the lower pole. The assumptions on which the method is based are perfectly plane discontinuity surfaces, continuous at least inside the blocks and characterized by a definite direction beforehand; nondeformable blocks; and the possibility of movement only without interference from adjoining blocks.

The block method distinguishes "indoor" rock-mass blocks (JB) from the blocks that overlook the digging surfaces (JP). The finite blocks can be either removable or nonremovable. Removable blocks are further divided into all identical stable blocks, stable blocks thanks to shear strength on discontinuities, and unstable blocks (key blocks). To define a finite and removable block stability condition, comparing acting and reacting forces is necessary. For this purpose, applying either an analytical or a graphic procedure is possible to define friction-angle values able to maintain a stable joints pyramid in connection with a potential sliding condition.

The ROCK3D (Geo&Soft, 2008) program is used for the block analysis and calculus, as stated previously. Using Goodman & Shi's (1985) key block theory, the calculus code recognizes possible kinematic mechanisms of blocks and estimates their stability in connection with extreme equilibrium. This analysis assumes that it is possible to associate a definite rock volume to every kinematic mechanism (release, sliding on one or two planes), even with a complex shape or bounded by different discontinuity planes and digging walls (if the discontinuity grid geometry allows that).

For a selected kinematic mechanism the program defines (according to the discontinuity tracks surveyed on the slope), the maximum close boundaries (which are not connected to each other), using only discontinuities that are connected and compatible with the examined kinematic mechanism. This analysis phase and the next phase must be repeated for every possible kinematic mechanism, looking for the greatest instability conditions. The program optionally generates a pseudorandom discontinuity map that respects the statistical distribution of frequencies and persistencies measured on the natural slope. In this way making a certain number of simulations is possible to anticipate the behavior of rock fronts before the on-site intervention. The next phase is directed to the complete geometrical reconstruction of complex blocks. The program defines the solid derived from the union of all elemental polyhedrons contained within close boundaries, eventually separated, identified in the following sections. For each complex block, ROCK3D calculates volumes and surfaces. The kinematic mechanism analysis, made using Goodman & Shi's (1985) block theory, allows us to associate every existing kinematic mechanism (release, sliding on one or two planes) and a definite rock volume, even with complex shape, if the discontinuity grid geometry allows that. The analysis used in this phase is divided into three phases:

(i) recognition of all rock pyramids created by the intersection of families of discontinuity planes;

(ii) recognition of rock pyramids that, in association with externally applied strengths, may possibly move; and

(iii) recognition of the removable blocks in connection with the previous ones that, according to their position, may be in critical stability conditions.

## 6.2 Results

The application of the key block theory in this work has determined the following results. The rock slope has been divided into six detailed areas and in two domains (northern front and southern slope), according to the results of in situ surveys as reported in the previous chapter. The space pyramid projections obtained in the two domains are reported in Fig. 10 for all the analyzed areas.

In all analyzed areas, the most common kinematic is determined by the intersection between two subvertical joint sets, K2 and K4 (in some cases K3 can replace K4, isolating similarly shaped blocks), and at the base cut by bedding plane (K1). Those blocks are denominated key blocks as 100, in other words under discontinuity K1 and above K2 and K3, as shown in Fig. 11. The same figure also shows, depending on the inclination of the intersection line between K2 and K4, that owing to verticality the block could plunge downhill or uphill and that it could slide on the intersection line or topple. The described phenomena can be observed in several cases on the slope.

Other kinds of removable blocks are determined by the key block method, but their JP are completely within the reference circle, indicating that their movement direction could only have been upward and, consequently, that instability could not occur under pure gravity.

Finally, one could observe that if weathering effects occur on the bedding planes, the movement of other block types could be determined by different key block types, which should be considered in the design of mitigation measurements.

Table 2 reports the block types computed for the six areas. Where the numbers 0 and 1 represent the block position below or above the discontinuity respectively. Block dimension is strongly influenced by spacing that averages between 10 and 25 cm, with maximum values of 50–60 cm.

## 7 Rockfall analysis

For the bidimensional analysis of the motion of single blocks traveling downslope, the calculation methodology proposed by Pfeiffer and Bowen (1989), who introduced it in the numerical code CRSP, has been chosen. This numerical program was developed in 1989 at the Colorado School of Mines, Department of Geology and Geological Engineering, in collaboration with the Colorado Department of Highways. The CRSP code was based on the experiences of various authors (Ritchie, 1963; Piteau and Clayton, 1977) and was calibrated using several experimental results obtained from artificially induced rockfalls along unstable slopes located in West Rifle and the Colorado Canyons (Colorado, USA).

In order to describe the block movement along the slope, the numerical code applies the equation of the parabolic motion of a free-falling mass and the principle of total energy conservation. The analysis is carried out dynamically, as the motion parameters calculated at one step are applied to the following step and as the combined effects of free falling, rebound, rolling, and sliding are taken into account as well.

The analysis of the Campione del Garda slope has been performed along 15 different sections (Fig. 2). The sections have been carefully chosen by the analysis of the morphology of the territory. For each section, 500 numerical simulations have been performed; and a statistical analysis of the results has been applied in order to calculate the modal values of kinetic energy, rebound height, and travel length of the blocks (Fig. 12).

The starting point for the rockfall has been chosen conventionally as the highest point of each section. The restitution coefficients Kn e Kt (Giani, 1997) used for the rockfall analysis were assumed as follow:

- outcropping rock: Kn = 0.3 and Kt = 0.8 with a standard deviation (s.d.) of 0.02, and friction angle (ϕ) equal to 30° (s.d. of 2°);
- debris areas covered by vegetation: Kn = 0.2 and Kt = 0.4, (s.d. of 0.02), and friction angle (ϕ) equal to 40° (s.d. of 2°);
- debris areas without vegetation: Kn = 0.3 and Kt = 0.6 (s.d. of 0.02), and friction angle (ϕ) equal to 35° (s.d. of 2°).

The phenomenological features have been calibrated on the basis of the observation of the blocks surveyed at the slope foot.

The coordinates of the lines forming the slope profile and the restitution and roughness coefficients associated with each portion of the block path have been indicated in the input files. The starting horizontal and vertical velocities, computed on the base of detachments conditions, have been constantly assumed to be equal to 1 and 0.5 m/s. The block shape has been considered spherical, with a recurring diameter of 0.3 m for what is considered to be the traveled path (the 0.3 m diameter causes the longest path and therefore the widest hazard zones). For the kinetic energy calculation, the block that produced the least favorable results (i.e., the higher energy) was spherical with a 0.5 m diameter.

For each section, the velocities, rebound heights, and maximum, average, and minimum kinetic energies have been calculated; the cumulative probability distributions of the velocities, kinetic energies, and rebound heights have been drawn for each part of the slope section. The number of blocks that stop at each slope progressively have also been recorded (Fig. 13).

For each homogeneous area of the slope front, the predisposition to block detachment has been defined as well. The activity value (considering the five parameters indicated by the adopted methodology, RHAP), the total possible unstable elements, and the relative activity (computed by comparing different cell activity of the same slope) have been determined for each investigated cell.

The activity value is considered low when <35%, medium between 35% and 60%, and high >60%. These degrees of activity, determined for the three different areas, resulted in 64%, 61%, and 64%, respectively, characterizing the whole front as being of "high" activity.

The hazard zonation has been obtained using the values of the hazard classes, determined on the basis of block arrest and transit percentages, increased by 1 as the activity of the front classified as "high." (Fig. 14).

## 7.1 Mitigation measures

Several defensive systems were evaluated in order to reduce the hazard zones on the basis of the accomplished results. Various typologies have been examined. Those that would better fit the area are described below. For this purpose the whole town of Campione del Garda has been divided the following several sectors (Fig. 15):

(i) *northern zone, Gardesana tunnel exit*: the existing tunnel should be lengthened at least 50 m outside the rock front and should be covered with 1 m of debris. The tunnel should be designed to face impacts of 600 kJ of energy. The rock block for the design should be considered spherical with a 0.5 m diameter as observed in situ;

(ii) *northern zone, embankment area*: the embankment, 4.5 m high, should be placed along the side of the rock front, protecting the Gardesana State Road. This embankment should begin directly at the side of the tunnel exit and should cover the whole area subjected to the risk. The area behind the embankment should be prohibited to people, and the ground should be ploughed for the first 0.5–1 m in order to soften it and increase its energy absorption capacity. The maximum energy for impact on the embankment should be considered equal to 250 kJ;

(iii) *central zone, cemetery proximity*: this area is the most difficult to protect, owing to the presence of structures in close proximity to the rock front and directly reachable by falling blocks (cumulative probability of about 50%). The installation of high-energy-absorption rockfall barriers allows for a reduction of the rockfall-induced risk. The maximum impact energy is equal to 1000 kJ, and the barrier height should be equal to 5 m;

*(iv) central and southern zones, between the cemetery area and the southern tunnel:* this area should be protected with an embankment 6 m high, which should be placed along the front edge of the rock, protecting a road. This embankment should begin directly adjacent to the southern tunnel entrance and cover the whole area subjected to rockfall-induced risk. The area behind the embankment should be prohibited to people, and the vegetation

should be preserved because it helps in the reduction of impact energy. The maximum impact energy calculated for the embankment is equal to 250 kJ; and

*(v) southern zone, tunnel entrance:* the existing tunnel (the northern tunnel) should be lengthened to at least 30 m and should be covered with at least 1 m of debris. The impact energy calculated for the top of the tunnel is equal to 600 kJ. The shape of the design block should be considered spherical with a 0.6 m diameter as observed in situ.

A two-dimensional rockfall analysis by using CRSP code was performed that took into account the presence of the above-described protection systems. A new final hazard zonation was then calculated and is shown in Fig. 15, where reduction of the high hazard zone can be seen.

## 7.2 Monitoring systems

During the geomechanical survey of the cliffs overlooking the town of Campione del Garda, a few potentially unstable blocks of considerable dimensions were observed.

These blocks are beyond the scope of this study, as their fall would most probably trigger a wider rockslide. Owing to the dimensions of those blocks, any passive defensive system would not be economically practicable. Nevertheless, monitoring the stability of such blocks should be considered absolutely essential for the safety and protection of the Campione del Garda inhabitants and structures. Thus, in order to design an appropriate monitoring system, further studies should be undertaken.

# 8 Conclusions

The Campione del Garda coastal cliff area is subject to high hazard and risk owing to rockfall phenomena. This situation needs to be mitigated by proper defensive and reinforcing methods for protection of the inhabitants and the structures. The design of the mitigation interventions must be based on the area's risk zonation in order to identify the optimum systems and locations.

The assessment of absolute risk should be based on historical data and occurrences of these phenomena, which are not available for this area. Consequently, a relative hazard evaluation based on the RHAP and adopted by several Italian institutions has been chosen. A kinematic analysis based on rock-mass structure has been performed to compute the probability of block detections on the slopes. This analysis was conducted by applying the key block method, which allows identification of the types of possible instability and evaluation of the block volumes. A block-path probabilistic analysis was then performed on several potentially hazardous sections and a two-dimensional analysis was made using the CRSP method.

Zonation of the relative hazard indicated mitigation measures that need to be adopted: artificial gallery accessing road protections, walls to avoid access to high hazard areas, removal of unstable blocks and monitoring of possible zones of unstable slopes. Designs of these various measures could be based upon the quoted lumped mass analysis in terms of impact energy to be absorbed (for the gallery and the walls) and for the definition of the structural dimensions (e.g., the gallery lengths). A new hazard zonation was completed in consideration of the proposed mitigation measures for quantifying the final hazard potential for the coastal cliff.

## 9 References

Abellán, A., Vilaplana, J.M., Martínez J., 2006. Application of a long-range terrestrial laser scanner to a detailed rockfall study at Vall de Núria (eastern Pyrenees, Spain). Engineering Geology, 88, 136–148.

Agliardi, F., Crosta, G., 2003. High resolution three-dimensional numerical modelling of rockfalls. International Journal of Rock Mechanics and Minining Science, 40(4), pp. 455–471.

Alejano, L.R., Stockhausen, H.W., Bastante, F.G., Alonso, E., Ramíez-Oyanguren, P., 2008. ROFRAQ: an empirical method to estimate the risk of accidents due to rockfalls in quarries. International Journal of Rock Mechanics and Minining Science, 45(8), pp.1252–1272.

Birch, J., 2006. Using 3DM analyst mine mapping suite for rock face characterization. In Tonon, F., Kottenstette, J. (Eds.). 41st U.S. Rock Mechanics (ARMA) Symposium Laser and Photogrammetric Methods for Rock Face Characterization. Golden, Colorado (USA). pp. 13-32.

Canuti, P., Casagli, N., Tarchiani, U., 1998. Rock fall hazard in coastal cliffs. Proceedings of 8th IAEG Congress, Vancouver,. Balkema Ed., Rotterdam, The Netherlands, pp. 1585–1592

Cassinis, G., Vercesi, P.L., 1982 - Lineamenti strutturali fra la Val Trompia e la Val Sabbia (Brescia) durante il tardo Trias ed il Giurassico inferiore. Boll. Soc. Geol. It., 101, pp. 317-326.

Castellarin, A., 1982. Lineamenti ancestrali sudalpini. In Castellarin, A., Vai, G.B. (Eds.): Guida alla Geologia del Sudalpino centro-orientale. S.G.I., Guide Geol. Reg., pp. 41-55.

Crosta, G.B., Agliardi, F., 2003. A new methodology for physically based rockfall hazard assessment. Natural Hazards Earth System Science, 3(5), pp. 407–422.

Dorren, L.K.A., 2003. A review of rockfall mechanics and modelling approaches. Proceeding in Physical Geography, 27 (1), pp. 69–87.

Dussauge, C., Helmstetter, A., Grasso, J.R., Hantz, D., Desvarreux, P., Jeannin, M., Giraud, A., 2002. Probabilistic approach to rock fall hazard assessment: potential of historical data analysis. Natural Hazards Earth System Science 2, pp. 15–26.

Ferrero, A.M., Forlani, G.F., Roncella R., Voyat, H.I., 2009. Advanced Geostructural Survey Methods Applied to Rock Mass Characterization. Rock Mechanics and Rock Engineering, 42(4), pp. 631-665.

Fisher, M., Bolles, R., 1981. Random Sample Consensus: A paradigm for model fitting with application to image analysis and automated cartography. Communication of the ACM, 24 (6), pp. 381–395.

Frattini, P., Crosta, G., Carrara, A., Agliardi, F., 2008. Assessment of rockfall susceptibility by integrating statistical and physically-based approaches. Geomorphology, 94 (3-4), pp. 419–437.

Geo&Soft., 2008. Key Block Theory Based on Three-Dimensional Rock Block Analysis. Rock3D. Manual. Available online in: http://www.geoandsoft.com.

Giani, G., 1997. Caduta massi: Analisi del moto ed opere di protezione. Ed. Hevelius, Benevento, Italy, 120 pp.

Giani, G.P., Giacomini, A., Migliazza, M., Segalini, A., 2004. Experimental and theoretical studies to improve rockfall analysis and protection work design. Rock Mechanics and Rock Engineering, 37(5), pp. 369–89.

Goodman, R.E., Shi, G.H., 1985. Block Theory and its Application to Rock Engineering. Ed. Prentice Hall,Englewood Cliffs, NJ, 338 pp.

Grun, A., 1985. Adaptive least squares correlations: a powerful image matching technique. South African Journal of Photogrammetry, Remote Sensing and Cartography, 14 (3), pp. 175–187.

Guzzetti, F., Reichenbach, P., Ghigi, S., 2004. Rockfall hazard and risk assessment along a transportation corridor in the Nera Valley, central Italy. Environmental Management, 34( 2), pp. 191–208.

Jaboyedoff, M., Dudt, J.P., Labiouse, V., 2005. An attempt to refine rockfall hazard zoning based on the kinetic energy, frequency, and fragmentation degree. Natural Hazards Earth System Science 5(5), pp. 621–632

Mazzoccola, D., Sciesa, E., 2001. La metodologia RHAP (Rockfall Hazard Assessment Procedure). Prevenzione dei fenomeni di instabilità delle pareti rocciose. Programme Interreg II C, pp. 84-95.

Okura, Y., Kitahara, H., Sammori, T., Kawanami, A., 2000. The effects of rockfall volume on runout distance. Engeeniring Geology 58(2), pp. 109–124.

Pfeiffer, T., Bowen, T., 1989. Colorado Rockfall Simulation Program. Boulder, Colorado (USA): Colorado School of Mines–U.S. Dept. of Transportation, Federal Highway Administration.

Pierson, L., Davis, S., van Vickle, R., 1993. The Rockfall Hazard Rating System Implementation Manual. Washington, USA: Oregon State Highway Division, Report FHWA-OR-90-01. Available online: http://tris.trb.org/view.aspx?id=459774

Piteau, D., Clayton, R., 1977. Discussion of paper "Computerized design of rock slope using interactive graphics for the input and output of geometrical data" by Cundall et al. Proceedings 16th Symposium on Rock Mechanics, ASCE, Minneapolis (USA), pp. 62-63.

Priest, S., Hudson, J., 1981. Estimation of discontinuity spacing and trace length using scanline surveys. International Journal of Rock Mechanics, Mining Sciences and Geomechanics Abstracts, 18(3), pp. 183–197.

Ritchie, A., 1963. Evaluation of rockfall and its control. Highway Research Record, National Research Council Washington D.C, no. 17, pp 13-28.

Roncella, R., Forlani, G., Remondino, F, 2005. Photogrammetry for geological applications: Automatic retrieval of discontinuity orientation in rock slopes. Videometrics IX—Electronic Imaging—IS&T/SPIE 17th Annual Symposium, pp. 17–27.

Schweigl, J., Ferretti, C., Nossing, L., 2003. Geotechnical characterization and rockfall simulation of a slope: a practical case study from south Tyrol (Italy). Engineering Geology, 67(3-4), pp. 281–296.

Vallet, J., Skaloud, J., Koelbl, O., Merminod, B., 2000. Development of a helicopter-based integrated system for avalanche and hazard management. Int. Archives of Photogrammetry and Remote Sensing, pp. 565–572.

Figure

Fig. 1. View of the Campione del Garda inhabited shore on the western coast of Lake Garda (Northern Italy).

Figure

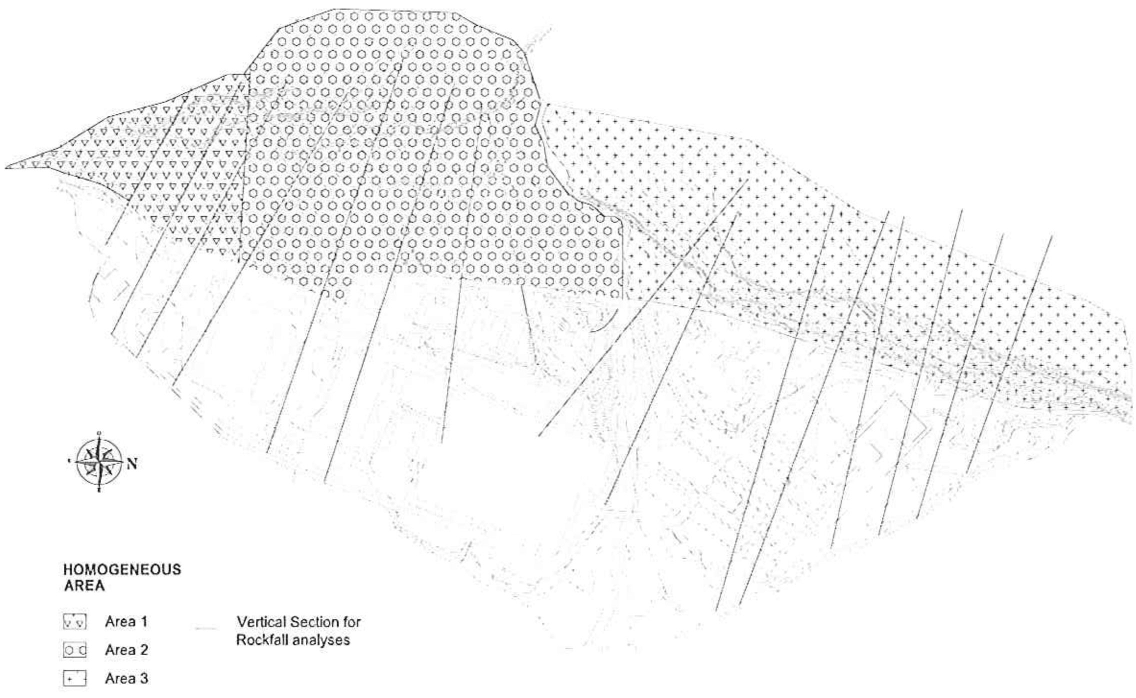


Fig.2. Definition of homogeneous areas on the base of the geomechanical characteristics of rock mass and traces of vertical sections utilized for rockfall analyses.

Figure

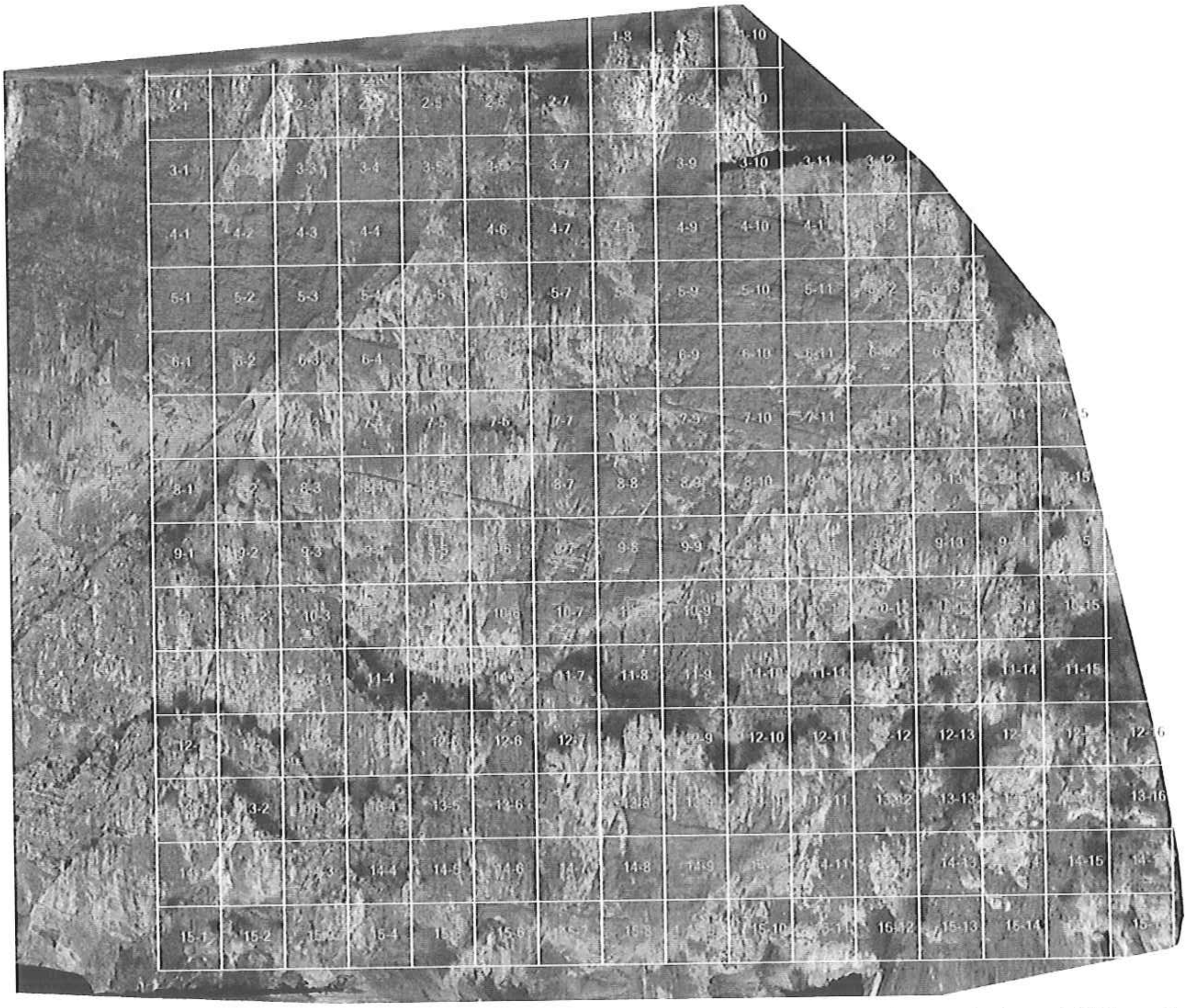

Fig. 3. Northern slope: square net utilized for the determination of the number of instability elements in the rockfall hazard zonation procedure.

**Figure**

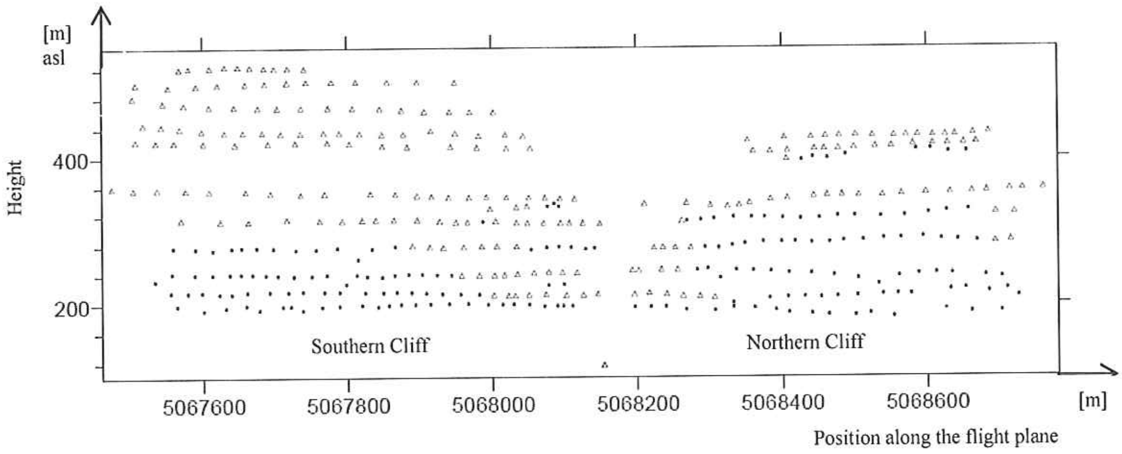


Fig.4. Shooting position during helicopter flight.

Figure

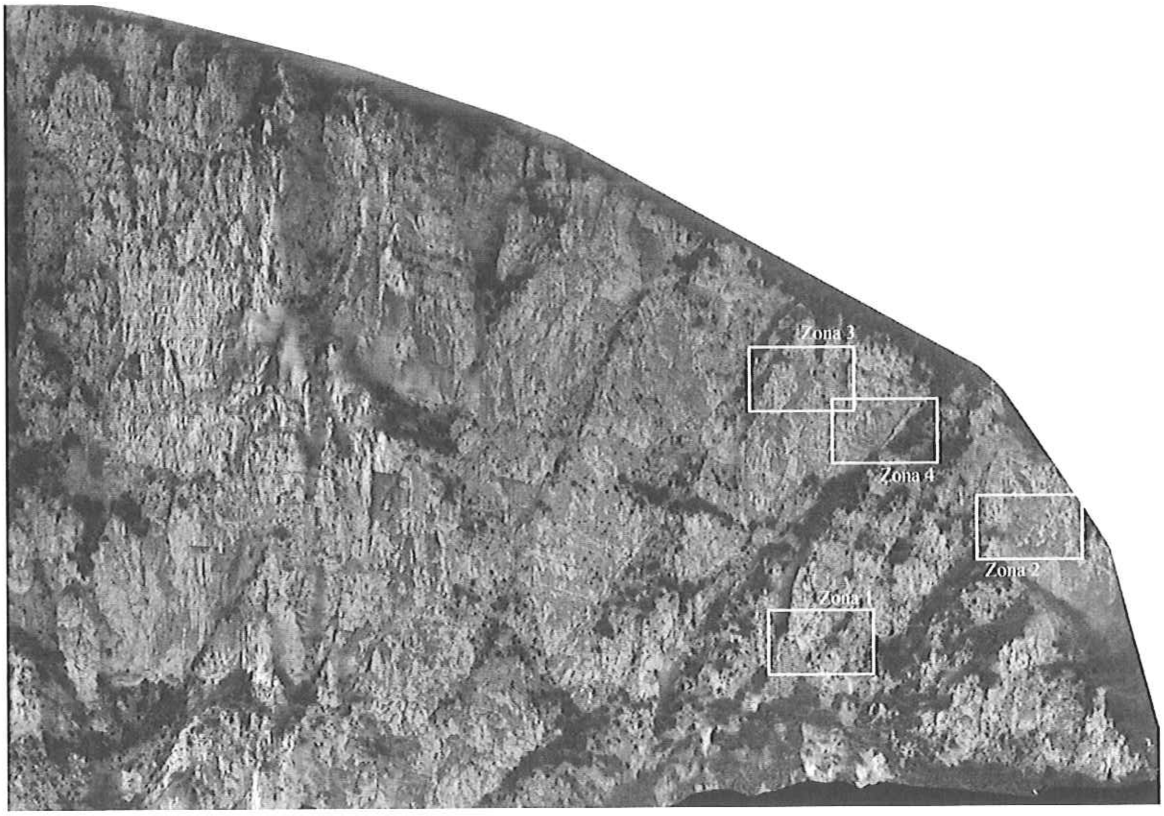


Fig. 5: South cliff orthophoto with indication of detailed areas.

Figure

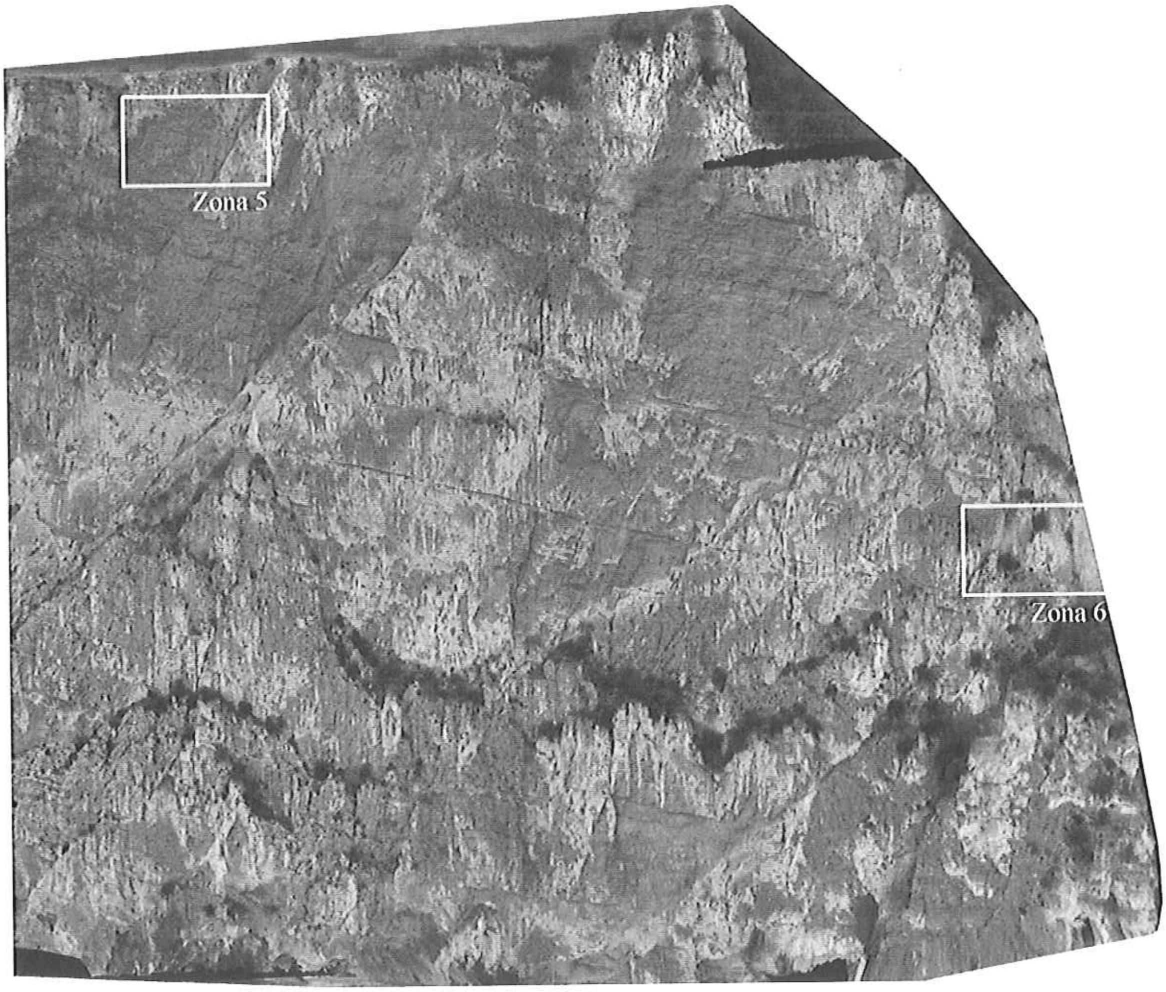


Fig. 6: North cliff orthophoto with indication of detailed areas.

Figure

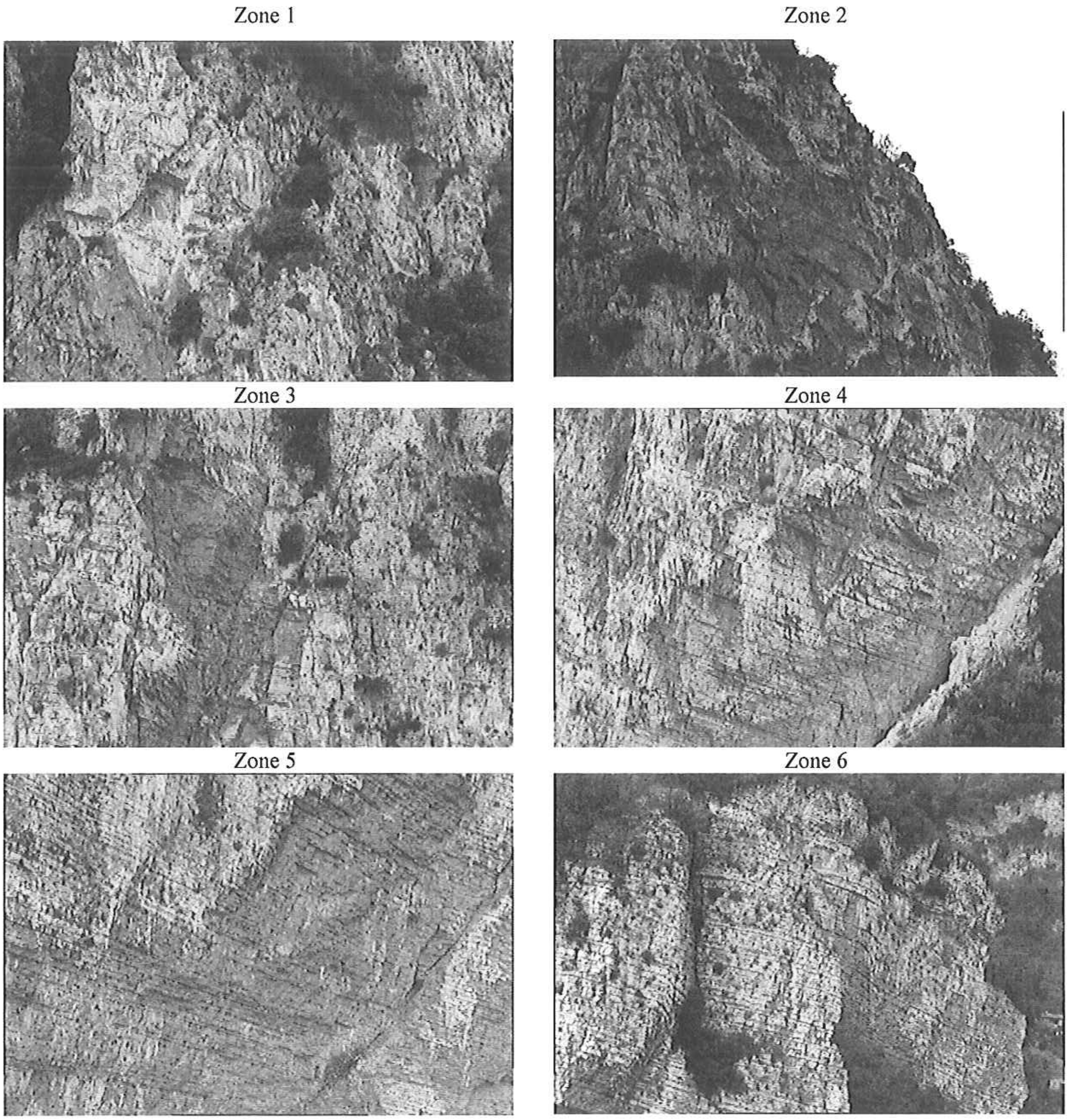


Fig. 7: Zones of detailed survey. Main Dolomite outcrop where apparent are the bedding strata and some vertical joints.

**Figure**

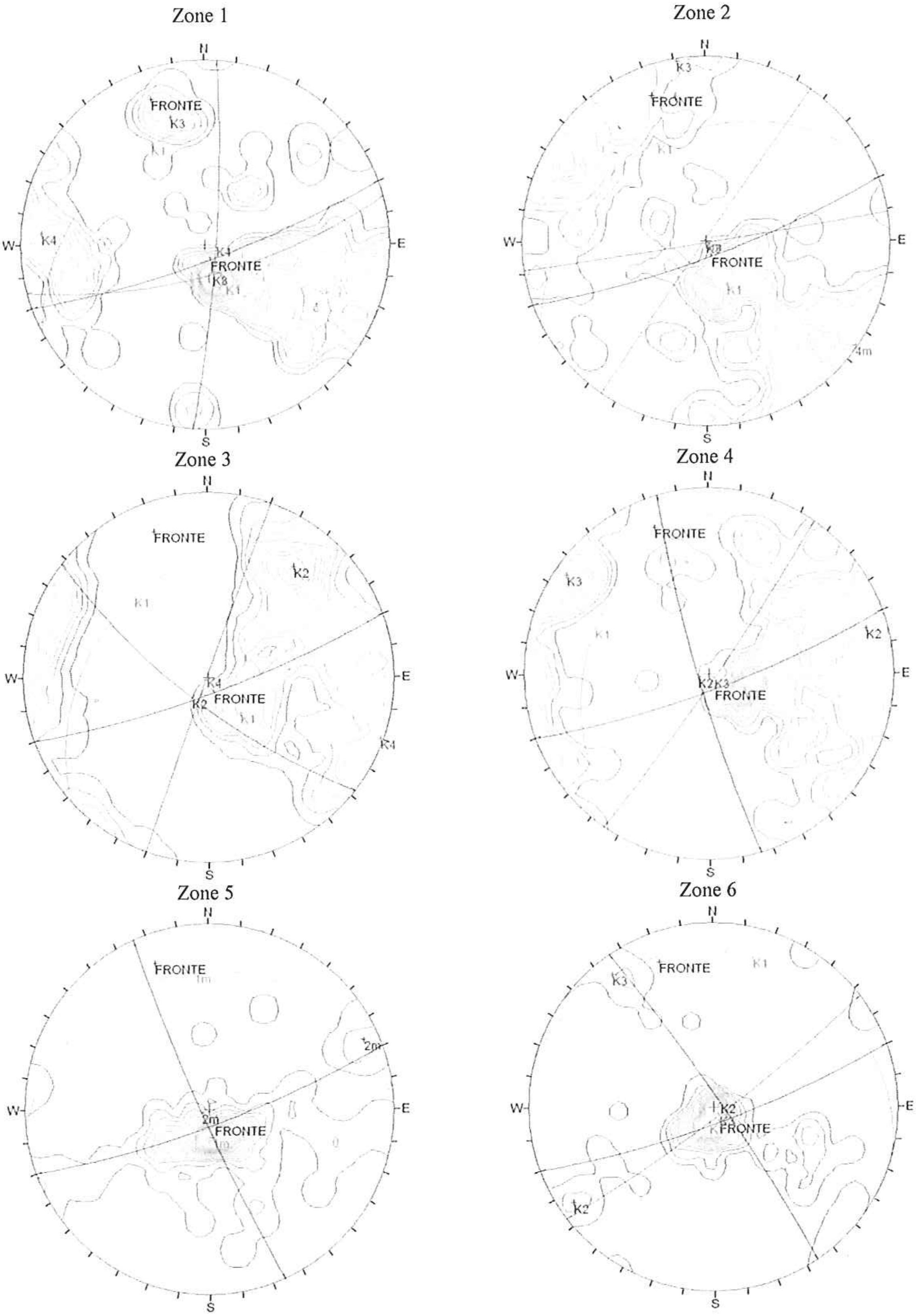


Fig. 8: Stereogram reproduction of the isocurves of measured poles and joint sets identified in each zone.

**Figure**

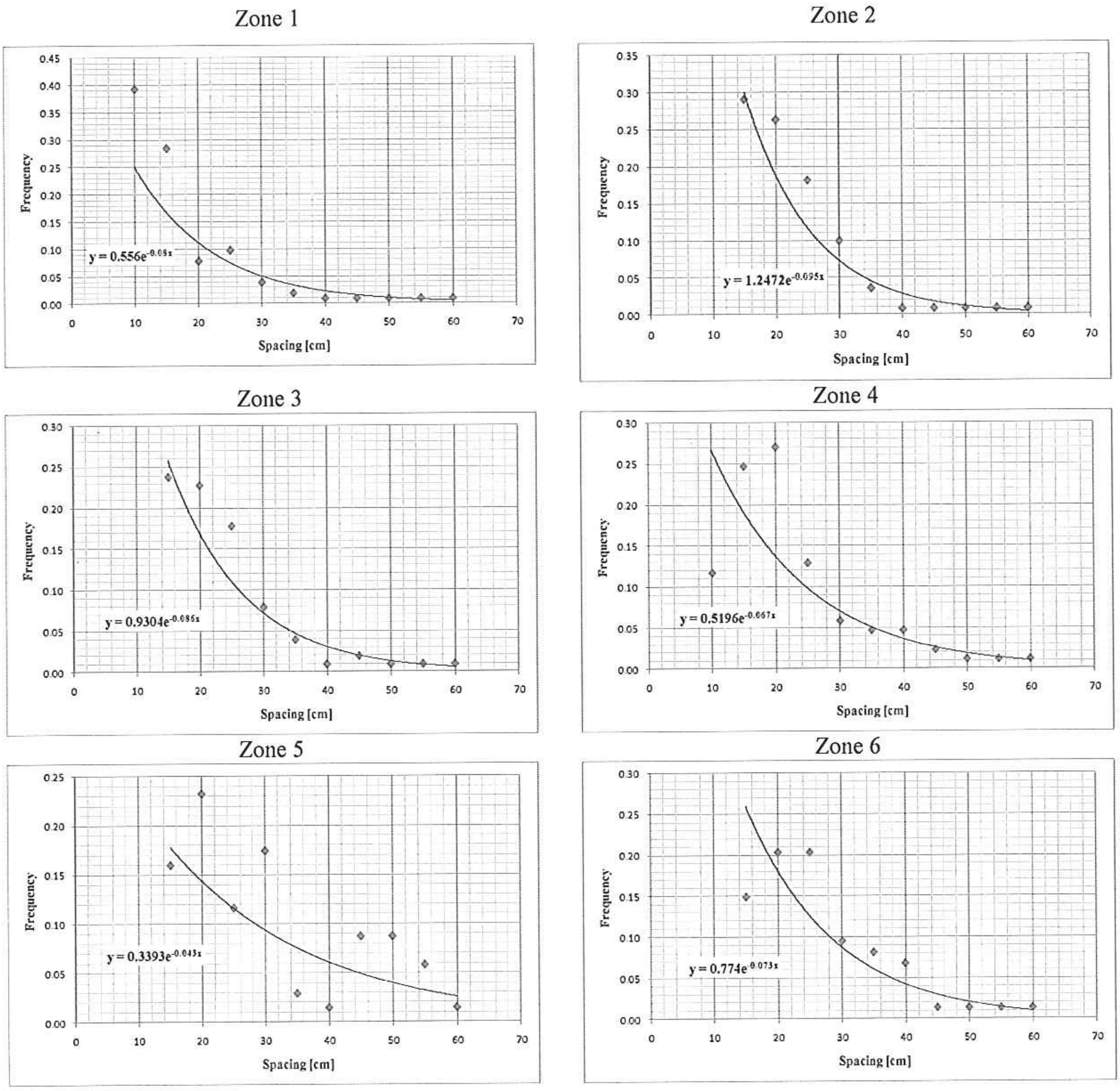


Fig. 9: Spacing distribution measured in each detailed zone.

**Figure**

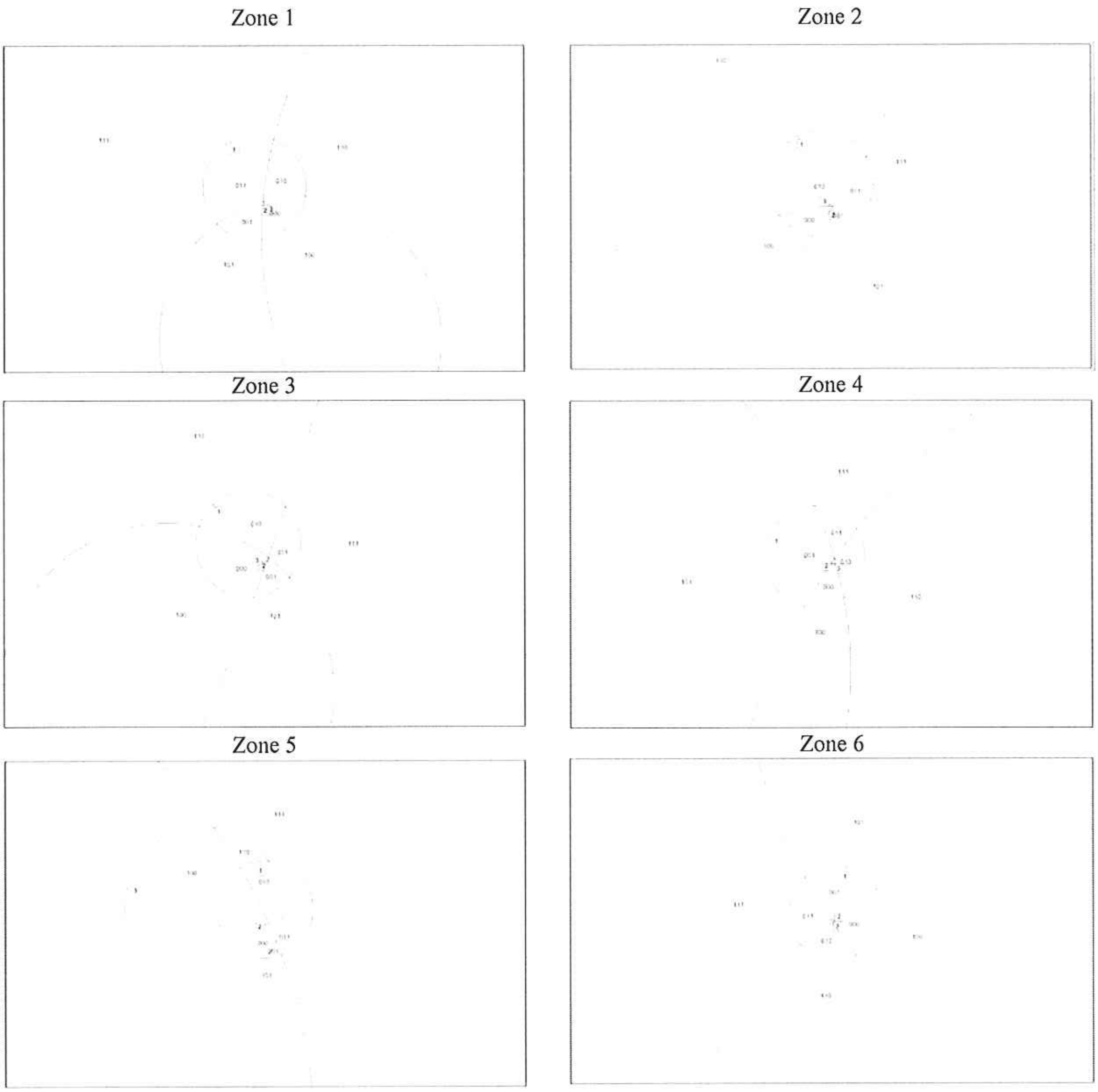


Fig. 10. Space pyramid projections computed in the six analyzed areas.

**Figure**

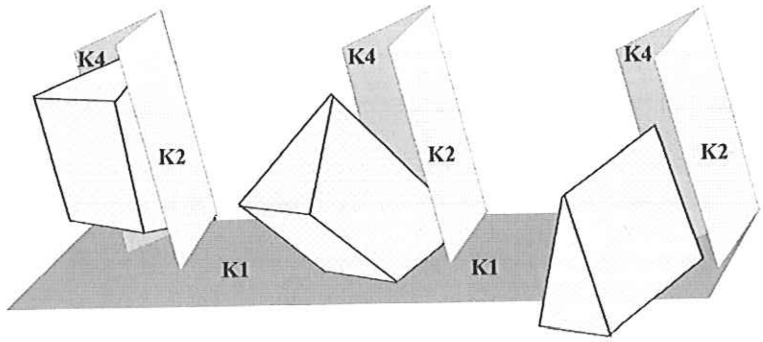


Fig.11. Schemes of computed instability phenomena.

**Figure**

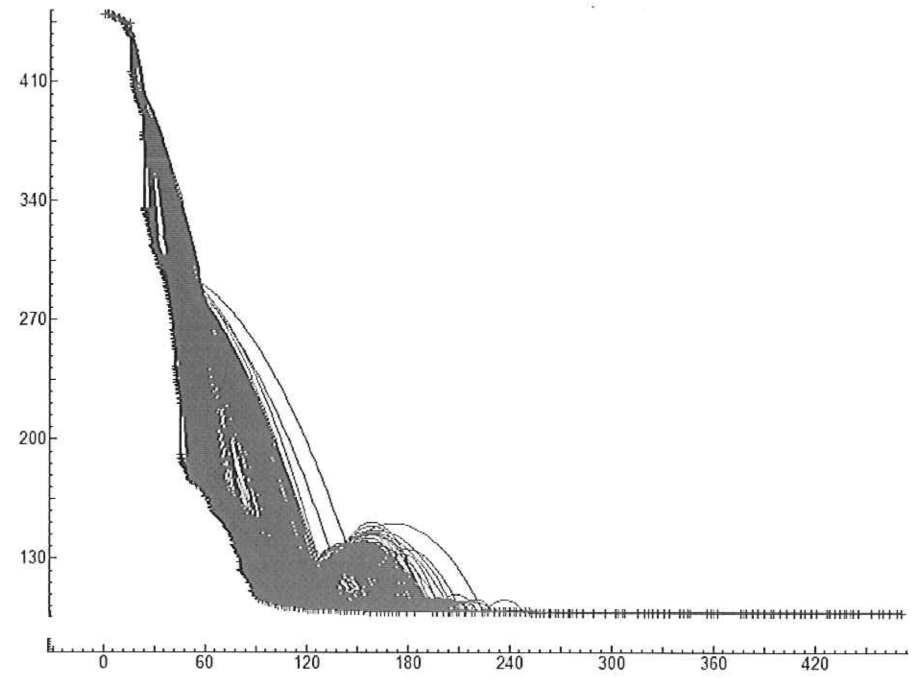


Fig. 12. Indication of the 500 analyzed paths in one analyzed section.

Figure

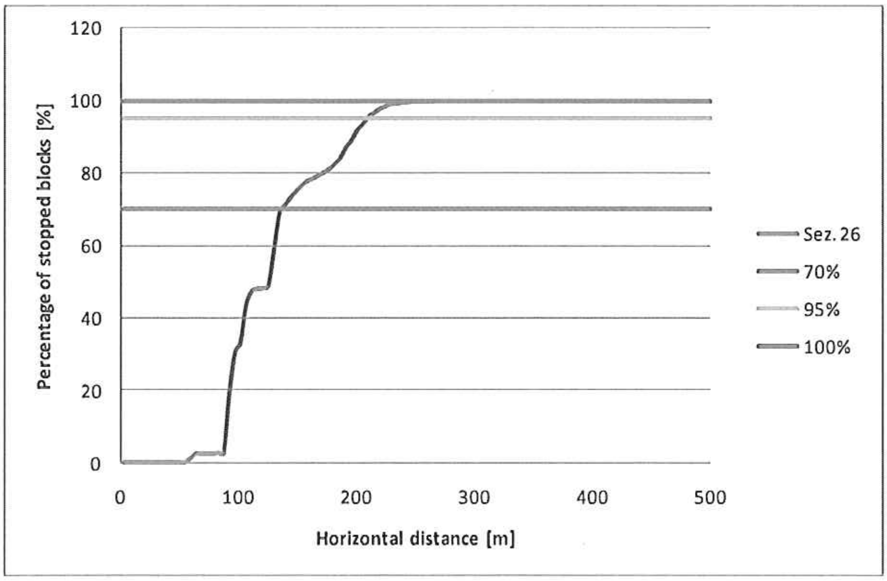


Fig. 13. Cumulative frequency of arrested block distance.

**Figure**

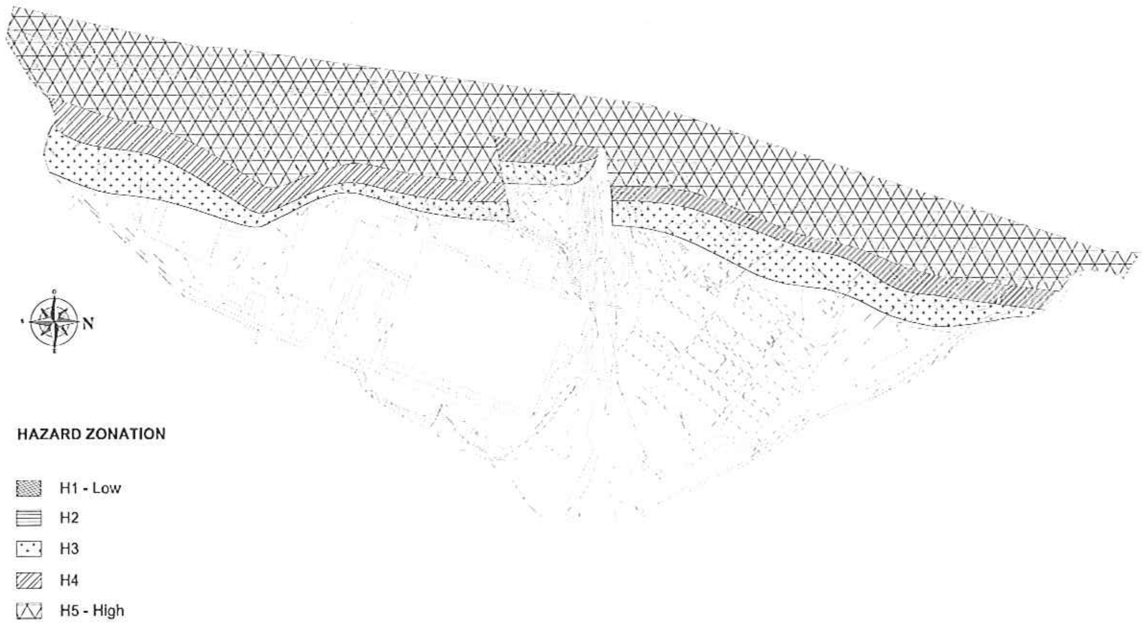


Fig. 14.Preliminary hazard zonation map. The lines indicate the 15 vertical sections along which rockfall were analyzed.

**Figure**

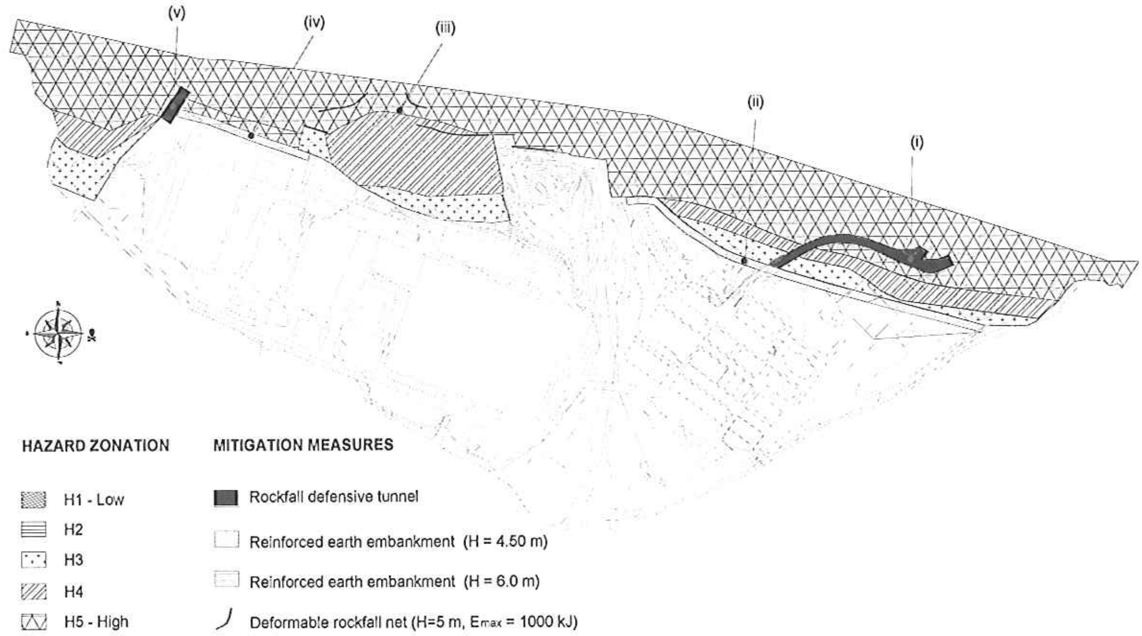


Fig. 15. Final hazard zonation map and indication of remedial works: (i) Gardesana tunnel exit; (ii) earth embankment with height of 4.5 m; (iii) deformable rockfall net; (iv) earth embankment with height of 6.0 m; (v) Gardesana tunnel entrance.

**Table**

| Discontinuity Sets | | Average orientation Dip [°] | Average orientation Dip direction [°] | Variability Dip [°] | Variability Dip direction [°] |
|---|---|---|---|---|---|
| South slope | K1 | 27 | 308 | 10–47 | 244–017 |
| | K2 | 73 | 221 | 58–88 | 200–240 |
| | | | | 85–88 | 026–059 |
| | K3 | 78 | 153 | 61–88 | 142–166 |
| | | | | 83–88 | 321–341 |
| | K4 | 89 | 295 | 72–88 | 272–318 |
| | | | | 72–88 | 090–135 |
| North slope | K1 | 13 | 360 | 0–35 | 015–270 |
| | K2 | 89 | 243 | 74–86 | 238–250 |
| | | | | 79–82 | 051–067 |
| | K3 | 84 | 143 | 75–87 | 141–150 |
| | | | | 83–85 | 315–320 |
| | K4 | 88 | 276 | 75–84 | 273–281 |
| | | | | 85–87 | 098–105 |

Table 1: Joint sets identified on South and North slopes, respectively.

**Table**

| Zone | Sliding | Falling |
|---|---|---|
| 1 | 100 | 000 |
| 2 | - | 001 |
| 3 | 101 | 001 |
| 4 | 100 | 000 |
| 5 | - | 001 |
| 6 | 110 | 010 |

Table 2. Key blocks computed for the six areas.